EUROPEAN ORGANIZATION FOR NUCLEAR RESEARCH
Laboratory for Particle Physics

Departmental Report

PHASE TRANSFORMATIONS DURING THE REACTION HEAT TREATMENT OF POWDER-IN-TUBE Nb_3Sn SUPERCONDUCTORS

M. Di Michiel[1], Ch. Scheuerlein[2]

The phase transformations prior to the superconducting A15 phase nucleation can influence the critical properties of fully reacted Nb_3Sn superconductors. We describe for the first time the phase transformations occurring during the heat treatment of state-of-the-art Nb_3Sn Powder-in-Tube strands, based on in-situ synchrotron diffraction measurements. All pure Sn present in the non-heat treated PIT strand is transformed into Cu_6Sn_5 by solid state diffusion. Subsequently $NbSn_2$ and Cu_6Sn_5 are partly transformed into a Sn-rich ternary Cu-Nb-Sn phase. When Sn starts to diffuse into the Nb tubes at about 520°C all Sn-containing phases are transformed into $NbSn_2$ and subsequently into Nb_6Sn_5.

1 European Synchrotron Radiation Facility (ESRF), Grenoble, France
2 CERN, Accelerator Technology Department, Geneva, Switzerland

Nb_3Sn strands of the Powder-In-Tube (PIT) design are considered for use in the next generation of high field accelerator magnets because they can provide high critical current and field, having at the same time a small effective filament diameter.[1,2] Recently, a PIT wire produced by ShapeMetal Innovation (SMI), in The Netherlands, in the framework of the EU-supported CARE/NED activity, has achieved a critical current density of 2500 A mm^{-2} at 12 T and 4.2 K with an effective filament diameter of 50 µm.[3]

In Nb_3Sn strands the superconducting A15 phase is produced during a reaction heat treatment (HT) in which the ductile precursor materials interdiffuse to form the brittle Nb_3Sn. The A15 phase microstructure and microchemistry in reacted Nb_3Sn strands has already been studied extensively with Scanning Electron Microscopy (SEM), using fracture samples and metallographic strand cross sections [4] and also with Transmission Electron Microscopy (TEM), using electron transparent lamellas produced by the Focused Ion Beam (FIB) technique.[5]

For Internal Tin (IT) Nb_3Sn strands the phase transformations occurring prior to Nb_3Sn nucleation and growth have also been studied using destructive methods,[6] but for PIT strands such results are still lacking. One reason for this is that in IT strands the Sn phases have cross sections of the order of several tens of µm^2, which allows to study these phases in metallographic strand cross sections using Energy Dispersive X-ray Spectroscopy (EDS) in the SEM, while the different Sn containing phases inside the Nb tubes have cross sections in the sub-µm range and, thus, their chemical composition can not be determined in the SEM.

Powder diffraction is an alternative method frequently used for phase analysis and the Nb_3Sn formation kinetics in strands of the IT design has been successfully studied by *in-situ* neutron diffraction. [7] However, the signal-to-noise ratio obtained by neutron diffraction experiments has not been sufficient to monitor the diffraction peaks of weekly diffracting phases, as for instance the orthorhombic $NbSn_2$ and Nb_6Sn_5.

Modern synchrotron sources can provide a high flux of monochromatic high energy x-ray beams, which can penetrate millimeter thick highly absorbing samples and which allow to record diffraction signals also from weekly diffracting phases with excellent statistics. In the present article we describe for the first time the phase transformations occurring during the reaction HT of a state-of-the-art Nb_3Sn PIT strand, based on x-ray diffraction (XRD) results that have been obtained at the ESRF High-Energy scattering beamline ID15B during *in-situ* reaction HT.

Two PIT strands manufactured by SMI have been studied. The strands contain up to 288 Nb-7.5wt.%Ta tubes with an approximate outer diameter of 50 µm, which are embedded in a high purity Cu matrix and which are filled with a powder containing $NbSn_2$ and Sn particles. The Cu that participates in the phase formations is mainly present in the form of a thin liner at the interface

between Nb-Ta tubes and powder. For more information about the PIT samples see references [1] and [3].

Diffraction experiments were performed in transmission geometry. The x-ray energy was 88.005 keV. Debye-Scherrer diffraction patterns have been acquired with a MAR345 image-plate detector. In-situ heat treatments were done in a dedicated furnace, which allows sample rotation during data acquisition. The accuracy of the sample temperature measurement is better than ± 10 °C over the entire temperature range. For phase identification the 2-D diffraction patterns acquired with the position sensitive detector were integrated into 1-D 2θ diffraction patterns. Phase identification has been done with the PANalytical Xpert software. The "allow pattern shift" option has been enabled in order to match peaks in the diffractograms acquired at elevated temperatures. The resolution of the experiment does not allow to distinguish between Nb, Ta and Nb-7.5 wt.%Ta. Cu has not been distinguished from α-bronze. Full structure refinement was not attempted. Instead diffraction peak areas are monitored for the determination of relative phase concentration changes. Prior to diffraction peak area measurements all diffractograms have been normalised by a constant so that their integrated intensity equals. This normalisation mainly compensates for beam current fluctuations during the *in-situ* HTs lasting up to 14 hours.

During *in-situ* HT with a ramp rate of 60 °C h^{-1} and isothermal heating for 4 h at 675 °C, a total of 85 diffractograms were acquired and all are summarised in Figure 1. Before the onset of Nb_3Sn formation after about 10 min heating at 675 °C, four phases (apart from Cu and Nb) could be identified, notably (β-) Sn, Cu_6Sn_5, $NbSn_2$ and Nb_6Sn_5. The presence of small amounts of other Cu-Sn intermetallics can not be excluded because the main Cu_3Sn and $Cu_{41}Sn_{11}$ peaks overlap with prominent peaks of other strand phases. A fifth phase was detected but could not be identified by comparison with reference diffraction pattern. It is assumed that this phase is a ternary Cu-Nb-Sn phase, which has been reported to appear during the reaction HT of IT strands with high Sn content.[8,9]

The first marked change in the diffractograms is the vanishing of the Sn reflections and the growth of the Cu_6Sn_5 pattern in the temperature range 160 °C-220 °C. When heating with a ramp rate of 60 °C h^{-1}, this transformation occurs entirely by solid state diffusion below the Sn melting temperature. $NbSn_2$ peaks are strongly decreased and the diffraction pattern of the presumed ternary Cu-Nb-Sn phase grows in the temperature range 370 °C-440 °C. The presumed ternary Cu-Nb-Sn phase disappears in the temperature interval 540 °C-560 °C upon formation of $NbSn_2$. At 650 °C $NbSn_2$ has been entirely transformed into Nb_6Sn_5, which is the only Sn containing phase detected at this temperature. After about 10 min 675 °C the Nb_3Sn reflections appear and during subsequent isothermal 675 °C HT Nb_6Sn_5 is entirely transformed into Nb_3Sn. A semi-quantitative description of the phase growth results is presented in Figure 2.

2

A second PIT sample was heated with a ramp rate of 300 °C h^{-1} to 490 °C and then cooled with a ramp rate of -300 °C h^{-1}. It can be seen in Figure 3 that above 370 °C the presumed Cu-Nb-Sn ternary phase grows continuously, mainly on the expense of $NbSn_2$, and it does not decompose upon cooling from 490 °C to room temperature. Solid Cu_6Sn_5 vanishes abruptly at 410 °C and re-appears upon cooling, again at about 410 °C. The diffractogram acquired at room temperature subsequent to the 490 °C HT is presented in Figure 4.

In Figure 5 the Nb_3Sn formation kinetics in the PIT strand at isothermal 675 °C HT is compared with the Nb_3Sn growth in an IT strand with low Sn content measured under identical experimental conditions.[10] It can be seen that unlike in the Nb_3Sn IT strand with low Sn content the Nb_3Sn phase formation in a PIT strand does not follow a parabolic growth law.

In summary, the phase transformations occurring during the reaction HT of PIT strands differ markedly from those in Nb_3Sn strands of the IT design. Because of the small cross sections of the phases involved, in the PIT strand pure Sn can be entirely transformed into Cu_6Sn_5 by solid state diffusion below the Sn melting temperature, which is impossible to achieve in IT strands within a reasonable duration. This implies that in the non heat treated PIT strand the Cu quantity inside the Nb tubes (including the Cu liner) must be at least 1.2 times the amount of pure Sn (in at.%).

However, there is not enough Cu inside the Nb tubes to transform all Sn into Cu_3Sn or more Cu rich Cu-Sn intermetallics. Therefore, when $NbSn_2$ and Cu_6Sn_5 decompose another Sn-rich phase must form. It is assumed that this phase is a ternary Cu-Nb-Sn phase. The approximate composition reported for the Cu-Nb-Sn ternary phase formed in an IT strand with high Sn content is 17 at.% Cu, 22at.% Nb and 61at.%Sn.[8] A ternary phase has also been observed in an IT strand produced by the so-called RRP process.[9] We have acquired diffraction pattern of the ternary phase in the RRP strand [11] and they match with the diffraction pattern of the presumed Cu-Nb-Sn phase in the PIT strand. It is thus concluded that the diffraction pattern of the Sn rich phase that is formed in the PIT strand upon Cu_6Sn_5 and $NbSn_2$ dissolution is characteristic for the Cu-Nb-Sn ternary phase reported in [8].

At about 520 °C Sn starts to diffuse into the Nb tubes forming $NbSn_2$. Simultaneously the Cu-Nb-Sn ternary phase vanishes and Nb is re-transformed into $NbSn_2$. At 620 °C the amount of $NbSn_2$ is about twice the amount of $NbSn_2$ powder in the strand prior to heat treatment (see Figure 2). At about 650 °C $NbSn_2$ is entirely transformed into Nb_6Sn_5 and during the subsequent isothermal 675 °C HT, Nb_6Sn_5 is successively transformed into Nb_3Sn.

Finally, the A15 phase growth in PIT strands does not follow a parabolic law, as it would be expected for a fully diffusion controlled processes. This behaviour may be explained by the fact that because of the high Sn content in the PIT strand part of the Nb tube is first transformed into $NbSn_2$

and Nb_6Sn_5 [12], prior to Nb_3Sn formation. $NbSn_2$ formation has also been observed in an IT strand with high Sn content [11] while Nb_6Sn_5 formation has not been reported for IT strands.

Nb_6Sn_5 formation prior to Nb_3Sn formation is assumed to cause the growth of a coarse Nb_3Sn region that does not significantly contribute to the critical current of the strand. Therefore, it might be advantageous to avoid or at least to reduce the Nb_6Sn_5 growth in the PIT strand. The reason why Nb_6Sn_5 is formed in the PIT strand but apparently not in high Sn IT strands remains to be studied.
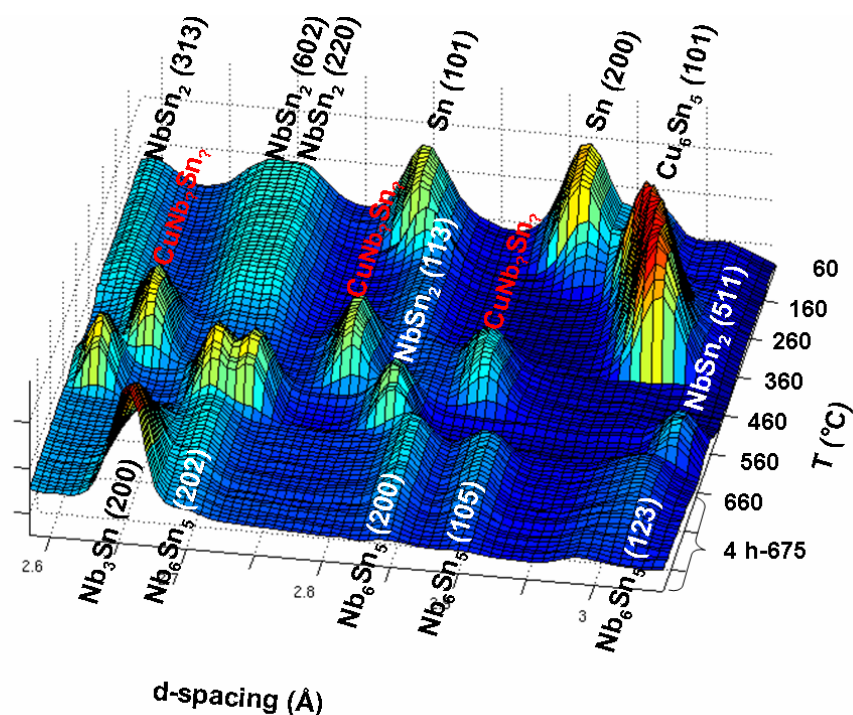
Figure 1: Summary of all diffraction pattern in the range 2.60 Å<d<3.05 Å acquired during the PIT reaction HT (ramp rate 60 °C h^{-1} to 675 °C and subsequent 4 h-675 °C isothermal HT). Diffractograms were acquired every 10 min, i.e. the temperature resolution of the experiment is 10 °C. The Sn containing phases that could be identified by comparison with reference diffraction pattern are pure Sn, Cu_6Sn_5, $NbSn_2$, Nb_6Sn_5 and Nb_3Sn. The presumed Cu-Nb-Sn ternary phase is indicated in red. Sn peaks vanish gradually below the Sn melting temperature, indicating that Sn is entirely transformed into Cu_6Sn_5 by solid state diffusion. Cu_6Sn_5 vanishes at about 410 °C. $NbSn_2$ peaks vanish while Nb_6Sn_5 appears between 640 °C and 650 °C. During the first hours of isothermal 675 °C HT Nb_6Sn_5 vanishes upon formation of Nb_3Sn.
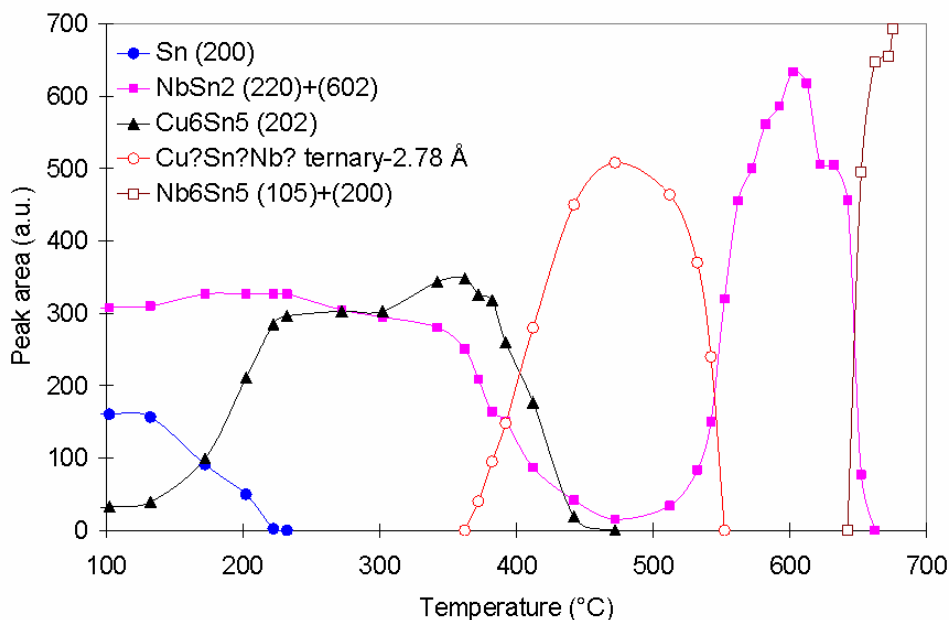

Figure 2: Relative variation of the diffraction peak areas of all Sn containing phases identified in the PIT strand as a function of the reaction heat treatment temperature (ramp rate 60 °C h^{-1}). Peak areas have been scaled in order to fit into the plot and to facilitate comparison. For the presumed ternary phase that did not match with published reference pattern the reflection at d ~2.78 Å has been used for peak area measurements.
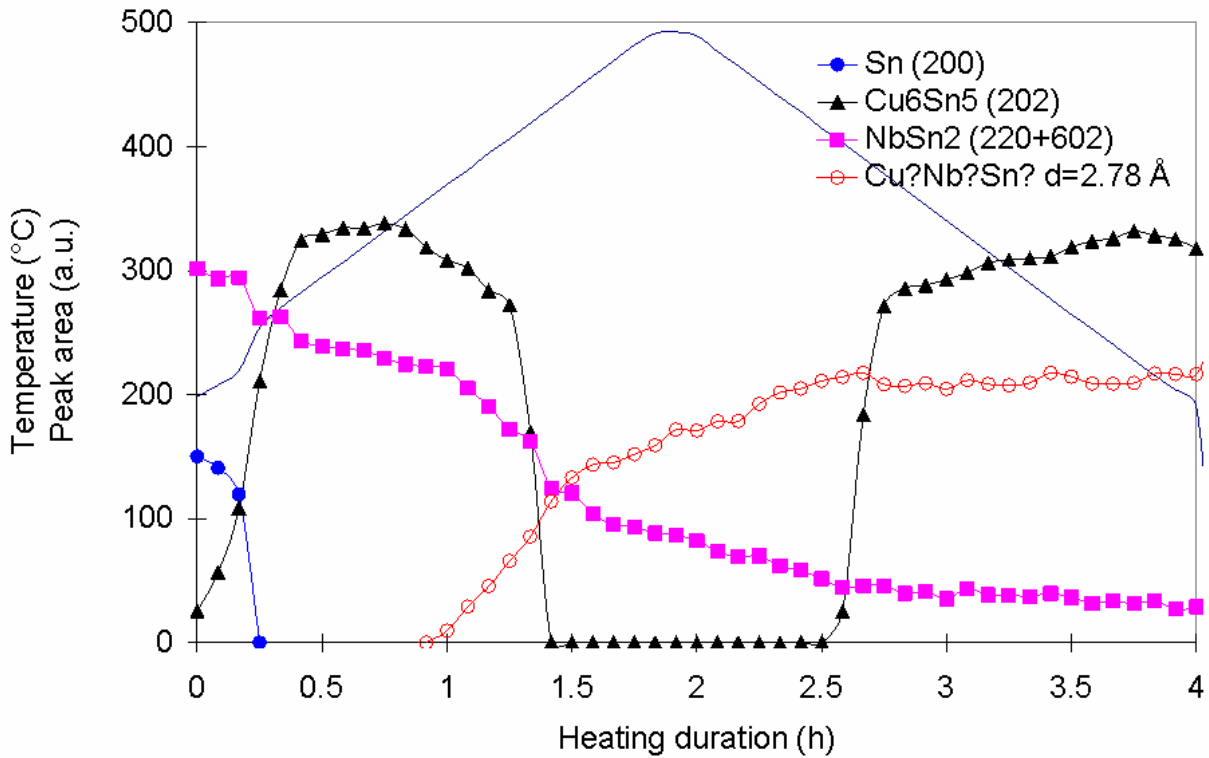
Figure 3: Relative variation of the diffraction peak areas of all Sn containing phases identified in the PIT strand during heat treatment cycle with a ramp rate of 300 °C h^{-1} up to 490 °C and subsequent cool-down with -300 °C h^{-1}. Peak areas have been scaled in order to fit into the plot and to facilitate comparison. The Cu-Nb-Sn ternary phase dose not decompose upon cooling from 490 °C to room temperature. The sample temperature is indicated by the continuous line without dots.
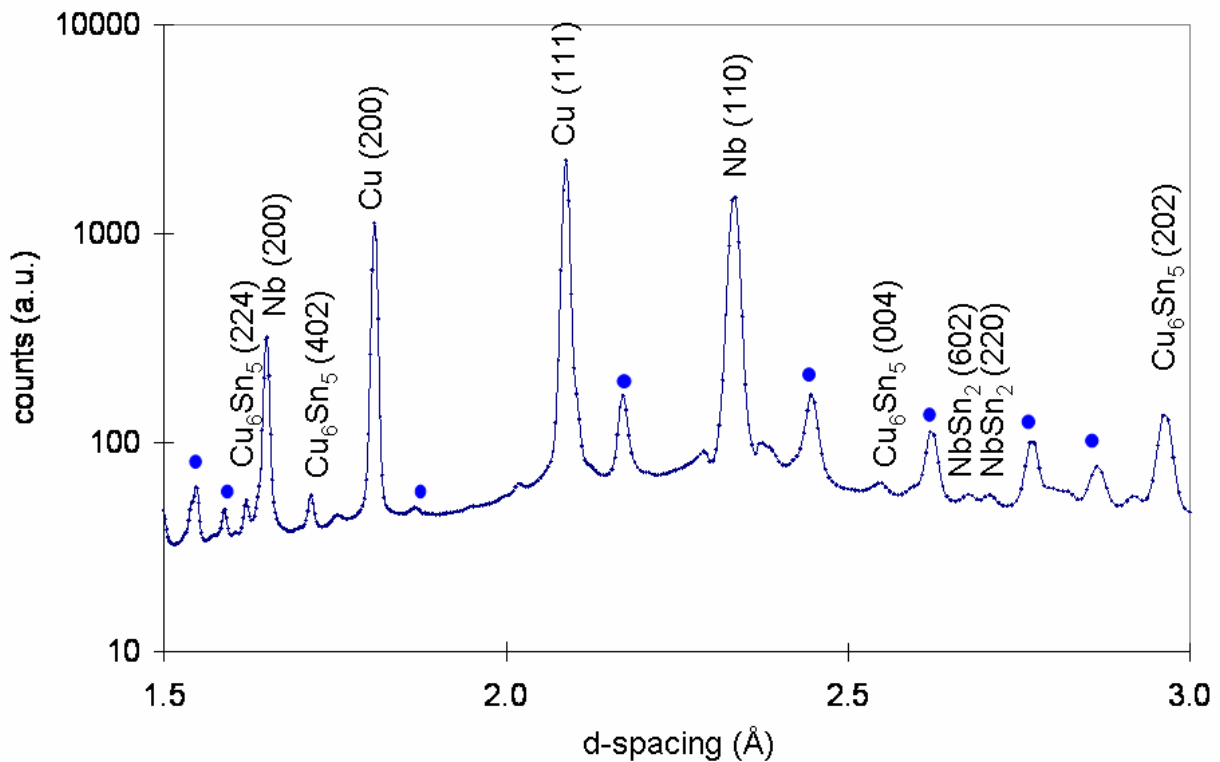

Figure 4: Diffractogram of the PIT strand acquired at RT subsequent to the 490 °C HT. The diffraction peaks of the Cu-Nb-Sn phase are indicated by full dots.
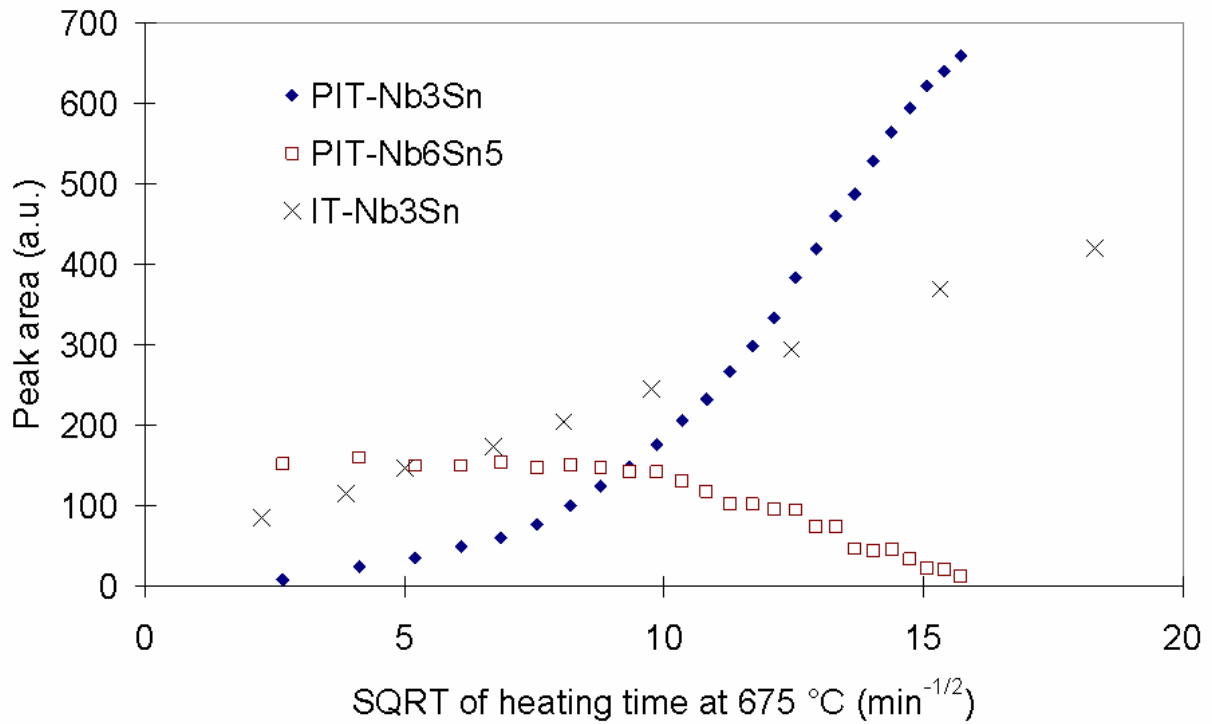
Figure 5: Nb_6Sn_5 (105)+(200) and Nb_3Sn (200) peak areas of the PIT strand as a function of isothermal 675 °C HT duration. For comparison the Nb_3Sn growth in an IT design strand with low Sn content is included in the plot. Unlike in the PIT strand, in the IT strand the Nb_3Sn growth during the first hours 675 °C HT follows a parabolic law.

References

[1] J.L.H. Lindenhovius, E.M. Hornsveld, A. den Ouden, W.A.J. Wessel, H.H.J. ten Kate, IEEE Trans. Appl. Supercon., vol. 10(1), 2000, pp. 975-978

[2] A. Devred et al., Supercond. Sci. Technol. 19, (2006), 67-83

[3] "*Industrially-Produced Nb₃Sn wire for NED achieves 1400 A at 4.2 T and 12 K*", CERN weekly bulletin 43/2006, (2006)

[4] C.D. Hawes, P.J. Lee, D.C. Larbalestier, Supercond. Sci. Technol. 19, (2006), 27–37

[5] P.-Y. Pfirter, M. Cantoni (dir), MSc thesis, EPFL Lausanne, (2006)

[6] M.T. Naus, P.J. Lee, D.C. Larbalestier, *IEEE Trans. Appl. Supercon.*, vol. 10(1), 2000, pp. 983-987

[7] M. Al-Jawad, P. Manuel, C. Ritter, S. H. Kilcoyne, J. Phys.: Condens. Matter, 18, (2006), 1449-1457

[8] M.T. Naus, PhD thesis, University of Wisconsin, (2002)

[9] J.A. Parrell, Y. Zhang, M.B. Field, P. Cisek, S. Hong, IEEE Trans. Appl. Supercon. 13(2), (2003), 3470-3473

[10] C. Scheuerlein, M. Di Michiel, A. Haibel, Applied Physics Letters, 90(12), 132510, (2007)

[11] C. Scheuerlein, M. Di Michiel, G. Arnau, L. Oberli, CERN AT/MCS internal note (2007)

[12] W.L. Neijmeijer, B.H. Kolster, Z. Metallkde 78, (1978), 730-737